NeuroImage 114 (2015) 257–263

Contents lists available at ScienceDirect

NeuroImage

journal homepage: www.elsevier.com/locate/ynimg

Decreases in theta and increases in high frequency activity underlie associative memory encoding

Jeffrey A. Greenberg [a,1], John F. Burke [a,1], Rafi Haque [b], Michael J. Kahana [a], Kareem A. Zaghloul [b,*]

[a] Department of Psychology, University of Pennsylvania, 19104, USA
[b] Surgical Neurology Branch, NINDS, National Institutes of Health, 20892, USA

ARTICLE INFO

Article history:
Accepted 28 March 2015
Available online 8 April 2015

Keywords:
Episodic memory
Associative memory encoding
Subsequent memory effect
iEEG

ABSTRACT

Episodic memory encoding refers to the cognitive process by which items and their associated contexts are stored in memory. To investigate changes directly attributed to the formation of explicit associations, we examined oscillatory power captured through intracranial electroencephalography (iEEG) as 27 neurosurgical patients receiving subdural and depth electrodes for seizure monitoring participated in a paired associates memory task. We examined low (3–8 Hz) and high (45–95 Hz) frequency activity, and found that the successful formation of new associations was accompanied by broad decreases in low frequency activity and a posterior to anterior progression of increases in high frequency activity in the left hemisphere. These data suggest that the observed patterns of activity may reflect the neural mechanisms underlying the formation of novel item-item associations.

Published by Elsevier Inc.

Introduction

When searching our memory for previously experienced episodes, we rely on retrieval cues established during memory encoding to target the desired memory. These retrieval cues can be shaped by environmental context, internal mental states, or by associations formed between items or events. For example, one may associate a given restaurant with an important conversation with a colleague; subsequent visits to the same restaurant may easily prompt recollection of that same conversation. Several theories of memory encoding posit computational correlates underlying the formation of such associations (Norman and O'Reilly, 2003; McClelland et al., 1995), and associative memory encoding appears to occupy a specific type of processing in the human memory system (Kahana, 2012). Functional MRI studies provide empiric evidence for the anatomic locations where these processes take place. These studies implicate the hippocampus and the perirhinal cortex in binding conceptual representations across distal and closely interacting cortical regions, respectively (Davachi et al., 2003; Mayes et al., 2007; Dalton et al., 2013). Despite theoretical and experimental work, however, understanding the specific neural mechanisms that underlie how associative memory encoding is mediated by the brain still remains an unresolved question.

Direct intracranial recordings during paired associates memory tasks offer an experimental paradigm well suited to directly explore this issue (Caplan, 2005). Participants in paired associates tasks are instructed to form explicit associations between items and then attempt to recall one member of each pair when the other is provided as a cue. Combining paired associates tasks with subsequent memory effect (SME) analyses, in which neural activity is compared between successful and unsuccessful encoding (Paller and Wagner, 2002; Sederberg et al., 2003), can isolate the neural mechanisms responsible for forming associations (Caplan and Glaholt, 2007; Molle et al., 2002). Intracranial electroencephalography (iEEG) recordings offer a range of benefits when compared to fMRI in investigating the precise spatiotemporal changes underlying this process (Jacobs and Kahana, 2010), but SME analyses using human iEEG have not been previously performed during a paired associates task.

We address this here by investigating the changes in neural activity underlying the successful formation of explicit associations using iEEG recordings captured from subdural and depth electrodes as 27 patients with medically refractory epilepsy participated in a paired associates memory task. Previous studies investigating changes in episodic memory related changes in iEEG activity have linked successful encoding with both increases and decreases in oscillatory power in multiple frequency bands (Nyhus and Curran, 2010). Most episodic memory tasks require encoding of both items and associations, however, and it is unclear whether these discrepancies may be related to the cognitive demands specific to the encoding task (Hanslmayr and Staudigl, 2013). Here, we directly compared changes in low (3–8 Hz; theta) and high (45–95 Hz; high gamma) frequency oscillatory power during the successful and unsuccessful encoding of explicit associations in order to investigate the neural mechanisms that specifically underlie associative memory encoding.

Materials and methods

Twenty seven participants with medication-resistant epilepsy underwent a surgical procedure in which platinum recording contacts

* Corresponding author at: Surgical Neurology Branch, NINDS, National Institutes of Health, Building 10, Room 3D20, 10 Center Drive, Bethesda, MD 20892-1414, USA.
E-mail address: kareem.zaghloul@nih.gov (K.A. Zaghloul).
[1] Denotes equal contribution.

http://dx.doi.org/10.1016/j.neuroimage.2015.03.077
1053-8119/Published by Elsevier Inc.

Table 1
Patient demographics, behavioral performance, and electrode counts. The table shows the gender, age, the number of items seen during the paired associates task (# items), the percent recall, and the number of bipolar pairs of electrodes for each patient (#BPD). In addition, a hospital code for each patient indicates where data were collected: Thomas Jefferson University Hospital (T), the University of Pennsylvania (U), and the National Institutes of Health (N).

Patient	Gender	Age	# items	% correct	# BPD
T1	M	33	300	44.0	105
T2	M	23	148	39.2	109
T3	F	48	100	39.0	84
T4	M	33	200	72.0	46
T5	M	45	200	31.0	86
T6	M	23	200	75.5	78
T7	M	29	200	65.0	63
T8	F	20	700	77.9	126
T9	M	20	500	31.6	140
T10	M	50	200	26.5	105
T11	M	18	200	25.5	91
T12	M	57	100	12.0	50
U1	M	20	200	35.5	130
U2	M	37	200	18.5	123
U3	M	40	100	11.0	46
U4	F	25	100	13.0	160
N1	M	13	180	40.6	51
N2	F	52	300	26.3	54
N3	M	22	180	21.7	84
N4	M	49	360	14.4	52
N5	F	44	276	14.5	94
N6	M	31	120	83.3	151
N7	F	54	240	25.0	104
N8	F	25	240	24.6	71
N9	F	33	300	38.0	90
N10	M	40	240	25.42	91
N11	F	30	434	58.3	79

were implanted subdurally on the cortical surface, as well as deep within the brain parenchyma. In each case, the clinical team determined the placement of the contacts so as to best localize epileptogenic regions. Data were collected at three different facilities: Hospital of the University of Pennsylvania (UP; Philadelphia, PA), Thomas Jefferson University Hospital (TJ; Philadelphia, PA), and the Clinical Center of the National Institute of Health (NIH; Bethesda, MD). The research protocol was approved by the institutional review board at each hospital, and informed consent was obtained from the participants and their guardians. All patients participated in the paired associates task during their stay at these hospitals (see Table 1).

Paired associates task

In each trial of the paired associates task, patients were first shown a list of study word pairs, and then later cued with one word from each pair selected at random. Patients were instructed to recall each cue word's partner from the corresponding study word pair list. Lists were composed of four pairs of common nouns, chosen at random and without replacement from a pool of high-frequency nouns (http://memory.psych.upenn.edu/WordPools). Words were presented sequentially and appeared in capital letters at the center of the screen. During the study period (encoding), each word pair was preceded by an orientation stimulus (a row of capital X's) that appeared on the screen for 300 ms, followed by a blank interstimulus interval (ISI) of 750 ms with a jitter of 75 ms. Word pairs were then presented on the screen for 2500 ms, followed by a blank ISI of 1500 ms with a jitter of 75 ms. During the test period (retrieval), one randomly chosen word from each study pair was shown, and the participant was asked to recall the other word from the pair by vocalizing a response into a microphone. The length, in items, between the pair of words presented during study and the cue word given at retrieval varied and is termed the study-test lag.

Each cue word was preceded by an orientation stimulus (a row of question marks) that appeared on the screen for 300 ms, followed by a blank ISI of 750 ms with a 75 ms jitter. Cue words were then presented on the screen for 3000 ms, followed by a blank ISI of 4000 ms. Participants could vocalize their response any time during the recall period after cue presentation. Vocalizations were digitally recorded and then manually scored for analysis. Responses were designated as correct (and considered successfully encoded) if the correct word was retrieved following the cue. Participants could also respond with a word that was not paired with the cue (intrusions) or with the word 'pass' or with no vocalization (pass).

In the main analyses, we compared EEG power during the presentation of items between correct and pass trials, excluding all intrusions. See Fig. 1a for a visual representation of the paradigm. The primary contrast of interest is the comparison of correct recalls and incorrect recalls. However, because there are many ways in which the participant can make an

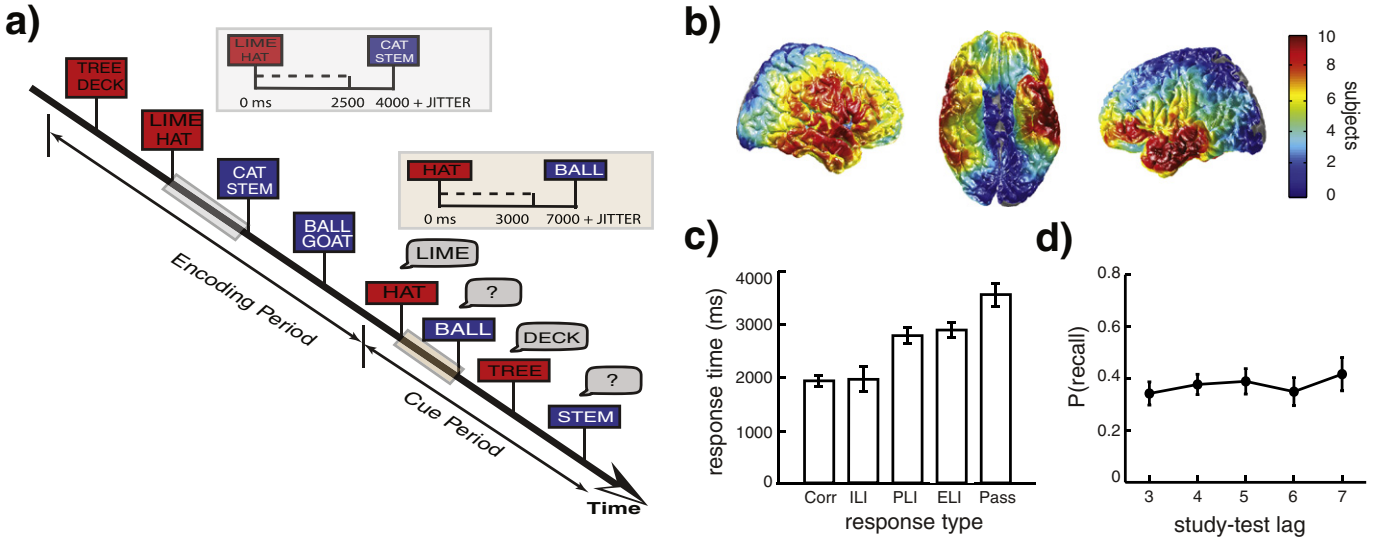

Fig. 1. a) Paired associates episodic memory task. In each trial, pairs of words are presented on the screen during encoding. Subsequently during retrieval, one word from each pair is randomly chosen and presented, and participants are instructed to vocalize the associated word. Timing of word and cue presentation are shown in the inset. b) Electrode coverage across all 27 participants. Colors correspond to the number of participants with electrodes contributing to each spatial region. Only anatomic regions with electrode contributions from at least five participants were included for group analyses. c) Mean response times in milliseconds, for each response type, across all participants. Error bars represent standard error of the mean. Bars represent response times for correct (Corr), intra-list intrusions (ILI), prior-list intrusions (PLI), extra-list intrusions (ELI), and pass trials. d) Probability of correct recall for all study-test lags averaged across all participants. Error bars represent standard error of the mean.

incorrect response in the paired associates task, we only consider an incorrect trial as one in which the participant did not make any response at all or vocalized a word to indicate they forgot the association (e.g. "pass"). Recalls in which the participant incorrectly retrieved a word that was not paired with the cue item (intrusions) were not considered in this analysis. Because, intrusions involve the retrieval of episodic associations, albeit the wrong associations, we omitted intrusions in order to explicitly examine the encoding mechanisms that support the subsequent retrieval of episodic associations.

Intracranial EEG recordings and bipolar electrode pairs

Data from our 27-patient database were collected in collaboration with three different hospitals. Whereas each hospital used the same general implantation procedures and data-acquisition techniques, our analysis had to account for technical details that varied by institution. Intracranial EEG (iEEG) data were recorded using a Nihon Khoden (TJ, NIH) or Nicolet (UP) EEG data acquisition system. Depending on the amplifier and the discretion of the clinical team, the signals were sampled at 400, 500, 512, 1000, or 2000 Hz. Signals were referenced to a common contact placed either intracranially or on the scalp or mastoid process. All recorded traces were resampled at 256 Hz, and a fourth-order 2-Hz stop-band Butterworth notch filter was applied at 60 Hz to eliminate electrical line noise. The testing laptop sent +/− 5 V analog pulses, via an optical isolator, into a pair of open lines on the clinical recording system to synchronize the electrophysiological recordings with behavioral events.

We collected electrophysiological data from subdural and depth recording intracranial contacts (AdTech; Racine, WI). Subdural contacts were arranged in both grid and strip configurations with an inter-contact spacing of 10 mm. Depth contacts (six to eight linearly arranged contacts spaced 6–8 mm apart) were placed in 13 out of 27 patients; all depth contacts were placed in the medial temporal lobe. Contact localization was accomplished by coregistering the postoperative computed tomographies (CTs) with the postoperative MRIs using FSL [FMRIB (Functional MRI of the Brain) Software Library] BET (Brain Extraction Tool) and FLIRT (FMRIB Linear Image Registration Tool) software packages. Preoperative MRIs were used when postoperative MRIs were not available. The resulting contact locations were mapped to both Montreal Neurological Institute (MNI) and Talairach space using an indirect stereotactic technique and OsiriX Imaging Software DICOM viewer package.

iEEG data were analyzed from bipolar pairs of electrodes in order to increase the signal-to-noise ratio of obtained recordings. Bipolar referencing is superior to the average referential montage in minimizing muscular artifacts in intracranial EEG (Kovach et al., 2011), and we used bipolar referencing to eliminate such confounds when analyzing the neural signal (Nunez and Srinivasan, 2006). We defined the bipolar montage in our dataset based on the geometry of iEEG electrode arrangements. For every grid, strip, and depth probe, we isolated all pairs of contacts that were positioned immediately adjacent to one another; bipolar signals were then found by differencing the signals between each pair of immediately adjacent contacts (Anderson et al., 2010; Burke et al., 2013). The resulting bipolar signals were treated as new virtual electrodes (henceforth referred to as electrodes throughout the text), originating from the midpoint between each contact pair. All subsequent analyses were performed using these derived bipolar signals. In total, our dataset consisted of 2463 bipolar electrodes (see Table 1 for a breakdown of the number of electrodes from each patient).

In order to identify and remove any artifacts in the recorded data, we applied a kurtosis threshold of 5 to the raw EEG data separately for each participant and electrode during each trial. Across participants, 87.3% ± .95% (mean ± SEM) of the experimental events remained after this artifact rejection procedure.

Data analyses and spectral power

To quantify memory-related changes in spectral power, we convolved the downsampled (256 Hz) bipolar iEEG signals with complex-valued Morlet wavelets (wave number 7) to obtain magnitude information (Addison, 2002). We used 30 logarithmically-spaced wavelets ranging from 2 to 95 Hz. We squared and log-transformed the magnitude of the continuous-time wavelet transform to generate a continuous measure of instantaneous power. We normalized power by *z*-scoring within each electrode and each frequency with respect to the mean and standard deviation of each experimental session. We focused our analysis on two bands: a low frequency activity (LFA) band (3–8 Hz, theta), and a high frequency activity (HFA) band (45–95 Hz, gamma).

To examine differences in spectral power during memory encoding, we averaged the instantaneous power across the encoding period for each word presentation (0–4000 ms relative to when the words appeared on the screen). For every electrode and encoding period, we calculated the difference in spectral power during memory formation (subsequent memory effect; SME) by calculating a *t*-statistic on the distribution of average power values associated with all successful and unsuccessful trials in both frequency bands. For all SME analyses, we defined unsuccessful trials as studied word pairs that did not elicit a correct response or intrusion at test.

To investigate the changes in spectral power during memory encoding in greater temporal detail, we binned the continuous-time instantaneous power into 600 ms epochs incremented every 80 ms starting 1000 ms before word onset and lasting until 4000 ms after word onset, yielding 56 total temporal epochs surrounding each stimulus presentation. 600 ms epochs were chosen so that each window contained at least one cycle of the lowest frequency analyzed (3 Hz). We averaged the instantaneous power over each bin.

Anatomical localization

To identify whether a particular anatomical area exhibited task-related changes in power, we grouped spatially similar electrodes from different participants into different anatomic regions. We segregated electrodes into seven anatomic regions, chosen based on their relevance to the task being analyzed (left and right frontal lobes, left and right temporal lobes, left and right medial temporal lobe regions that included the hippocampus, and a bilateral visual region) (Lancaster et al., 2000; Manning et al., 2011). All anatomic regions except the MTL region were defined using Brodmann Areas. The frontal lobe was defined as Brodmann Areas 9, 10, 11, 44, 45, 46, and 47; the temporal lobe was defined as Brodmann Areas 20, 21, and 22, and the visual region was defined as Brodmann Areas 17, 18, 19, and 37. For the MTL/hippocampal region, a clinician experienced in neuroanatomical localization manually reviewed postoperative CTs and MRIs to accurately identify all depth contacts located within the medial temporal lobe (Lega et al., 2011; Serruya et al., 2014). A bipolar electrode pair was categorized into an anatomic region if at least one contact within the pair was determined to lie within the structure.

For each patient and each of the seven anatomic regions, we obtained an average SME *t*-statistic for each region, temporal epoch, and frequency band by averaging the SME *t*-statistics across all individual electrodes located within that anatomic region. In order to determine whether a given anatomic region exhibited significant changes in activity across patients during successful memory encoding, we compared the distribution of SME *t*-statistics across patients for a given anatomic region and frequency band to zero using a paired *t*-test. We used a false discovery rate (FDR) procedure with $q = 0.1$ applied to all *p*-values from all anatomical regions to correct for multiple comparisons (Genovese et al., 2002).

To determine the spatial distribution of changes in low and high frequency power with successful memory encoding, we also created 760 smaller regions of interest (ROI) evenly spaced every 9.88 ± 1.26 mm

on the cortical surface of a Montreal Neurological Institute N27 standard brain. We grouped spatially similar electrodes from different participants by identifying electrodes that fell within 12.5 mm of each ROI. Only regions that had electrodes from five or more participants were included in this analysis (Fig. 1b).

In order to determine whether these smaller ROIs exhibited significant differences in spectral power between successful and unsuccessful memory encoding across participants, we used a permutation procedure. For every electrode in every participant, we calculated a *t*-statistic comparing the recalled and non-recalled distributions in low and high frequency power over the encoding period. We grouped electrodes within each ROI by taking the average of the *t*-statistics within participants, and then for each ROI calculated the summed *t*-statistic across all participants with electrodes in that ROI. We then permuted the trial labels for the trial types 1000 times and calculated a distribution of summed *t*-statistics across participants for each ROI. To generate a *p*-value for the differences in power for a given ROI, we determined the position of the true summed *t*-statistic in the distribution of permuted summed *t*-statistics. The permutation procedure thus decreases the influence of the number of patients on the *p*-value for any one ROI. As with the larger anatomic regions, we then used a false discovery rate (FDR) procedure with $q = 0.01$ applied to all *p*-values from all ROIs to correct for multiple comparisons (Genovese et al., 2002).

To visualize the spatially precise changes in spectral power across all participants, we identified ROIs that exhibited a significant ($p < 0.005$, FDR corrected across all ROIs) difference in spectral power between successful and unsuccessful memory encoding for each frequency band. Cortical topographic plots were rendered by assigning each vertex in the 3D rendered image of the standard brain the average *t*-statistic for that ROI across participants. All colored regions, independent of color intensity, identically indicate one-tailed significance at the $p < 0.005$ level as determined by the permutation procedure.

Results

Twenty seven participants with medication-resistant epilepsy who underwent a surgical procedure for placement of intracranial electrodes for seizure monitoring participated in a paired associates episodic verbal memory task during their hospital stay (Fig. 1a). Participants studied 235 ± 42 (mean ± SEM) word pairs. Participants successfully recalled 40.5% ± 5.7% words. On 9.8% ± 1.9% of trials, participants responded with intra-list intrusions (ILI). Participants responded with prior-list intrusions (PLI) on 2.7% ± 0.6% of trials and with extra-list intrusions (ELI) on 4.8% ± 1.4% of trials. All other study word pairs were not successfully recalled (the patient either made no response to the corresponding test probe, responded with a non-word vocalization, or said 'pass'). The mean response times across patients were 1930 ± 127 ms for correct responses, 2848 ± 153 ms for intra-list intrusions, 2864 ± 200 ms for prior-list intrusions, 2902 ± 194 ms for extra-list intrusions, and 3560 ± 220 ms for pass trials (Fig. 1c). A one-way repeated measures ANOVA revealed no significant main effect of the number of items presented between study and test (study-test lag) on recall probability (Fig. 1d; $F_{(4,56)} = 1.70$, $p = .16$).

In order to identify the neural mechanisms underlying the successful formation of associative memory, we calculated the difference in oscillatory power between successful and unsuccessful memory encoding for every frequency at every time point during encoding in each anatomic region (Fig. 2a). On average, across participants we observed that the largest differences arose in low (3–8 Hz; LFA) and high (45–95 Hz; HFA) frequency activity. To investigate these changes more rigorously, we focused our subsequent analyses on these two frequency ranges in seven anatomic regions across participants. Most anatomic regions exhibited a decrease in LFA across the encoding period during successful compared to unsuccessful memory encoding (Fig. 2b). Regions exhibiting significant decreases across all participants ($p < .05$, two-tailed, FDR corrected; two green asterisks in Fig. 2b) included the left frontal lobe ($t(12) = -3.99$, $p < .05$), the left temporal lobe ($t(15) = -4.61$, $p < .05$), and the bilateral visual region ($t(17) = -4.66$, $p < .05$).

We visualized the specific anatomic locations that exhibited significant changes in LFA between successful and unsuccessful memory encoding across participants (Fig. 2c; see Methods). We rendered all regions of interest (ROIs) exhibiting significant differences across participants ($p < 0.005$, permutation procedure; see Methods), where color intensity represents the average *t*-statistic across participants with electrodes in that ROI. As when examining anatomic regions, we found significant decreases in LFA in the left frontal and temporal lobes. Notably, we did find some ROIs with significant increases in LFA during successful memory encoding in the right temporo-parietal junction, although the number of regions was not large enough to generate significant differences when examining anatomic regions (Fig. 2b, c).

When we examined changes in high frequency activity, we found that most anatomic regions exhibited an increase in HFA across the encoding period during successful versus unsuccessful memory encoding (Fig. 2d). Regions exhibiting a significant increase across all participants ($p < .05$, two-tailed, FDR corrected; two green asterisks in Fig. 2d) were the left frontal lobe ($t(12) = 2.64$, $p < .05$), the left temporal lobe ($t(15) = 2.47$, $p < .05$), and the bilateral visual region ($t(17) = 6.08$, $p < .05$). The left MTL region also showed a reliable increase in HFA across subjects, but this difference did not survive FDR correction ($t(7) = 2.57$, $p < .05$; one green asterisk).

We also visualized the specific locations that exhibited changes in HFA across participants and found similar increases in the left frontal, left temporal, bilateral MTL and visual areas (Fig. 2e). We did note some specific areas with decreases in HFA in the right frontal lobe, the orbitofrontal cortex, and notably just anterior to the increases observed in the left temporal lobe. Again, these specific ROIs were not extensive enough to elicit changes in broader anatomic regions.

Because high frequency activity has been found to be highly correlated with single unit and BOLD activity (Mukamel et al., 2005; Manning et al., 2009; Ray and Maunsell, 2011b; Magri et al., 2012), we investigated HFA changes in greater temporal detail to identify networks involved in successful paired associates encoding (see Methods). For every temporal epoch and every anatomic region, we computed the average SME *t*-statistic across all participants to generate a detailed time course for changes in high frequency activity during successful encoding (Fig. 3a; red trace). We similarly examined the precise time course of LFA in all anatomic regions (Fig. 3a; green trace).

In order to assess whether changes in HFA and LFA exhibited a progression in time across anatomic regions, we examined the average time point where the SME reached its maximum value across participants. Specifically, we compared the times of peak differences in HFA power between successful and unsuccessful encoding by finding peaks in HFA *t*-statistics across time for each region. HFA peaked in the bilateral visual ROI at 971 +/− 251 ms, followed by peaks in the left MTL (1640 +/− 408 ms), the left temporal lobe (2079 +/− 252 ms), and the left frontal lobe (2373 +/− 209 ms; Fig. 3b, c, red trace). We performed a one-way ANOVA to test for differences in mean peak HFA time across the four regions of interest (bilateral visual, left MTL, left temporal, and left frontal) and found that across-subject mean peak HFA times differed significantly ($F_{(3,52)} = 6.37$, $p = .001$).

We performed post-hoc unpaired *t*-tests to directly compare the distribution of mean peak HFA times across participants. Post-hoc *t*-tests revealed that the left temporal and the left frontal lobes activated significantly after the visual regions during successful encoding ($p < 0.01$; see Fig. 3c). Furthermore, the left MTL trended to activate significantly before the left frontal region ($p < 0.1$). Overall, these timing analyses suggest that successful encoding occurs in two distinct networks: a posterior visual network that occurs very early after the presentation of items and a left frontal–temporal network that activates after the visual region. The left MTL appears to activate in between these two networks. Importantly, these data are consistent with similar findings using HFA to map memory encoding in free recall (Burke et al., 2014).

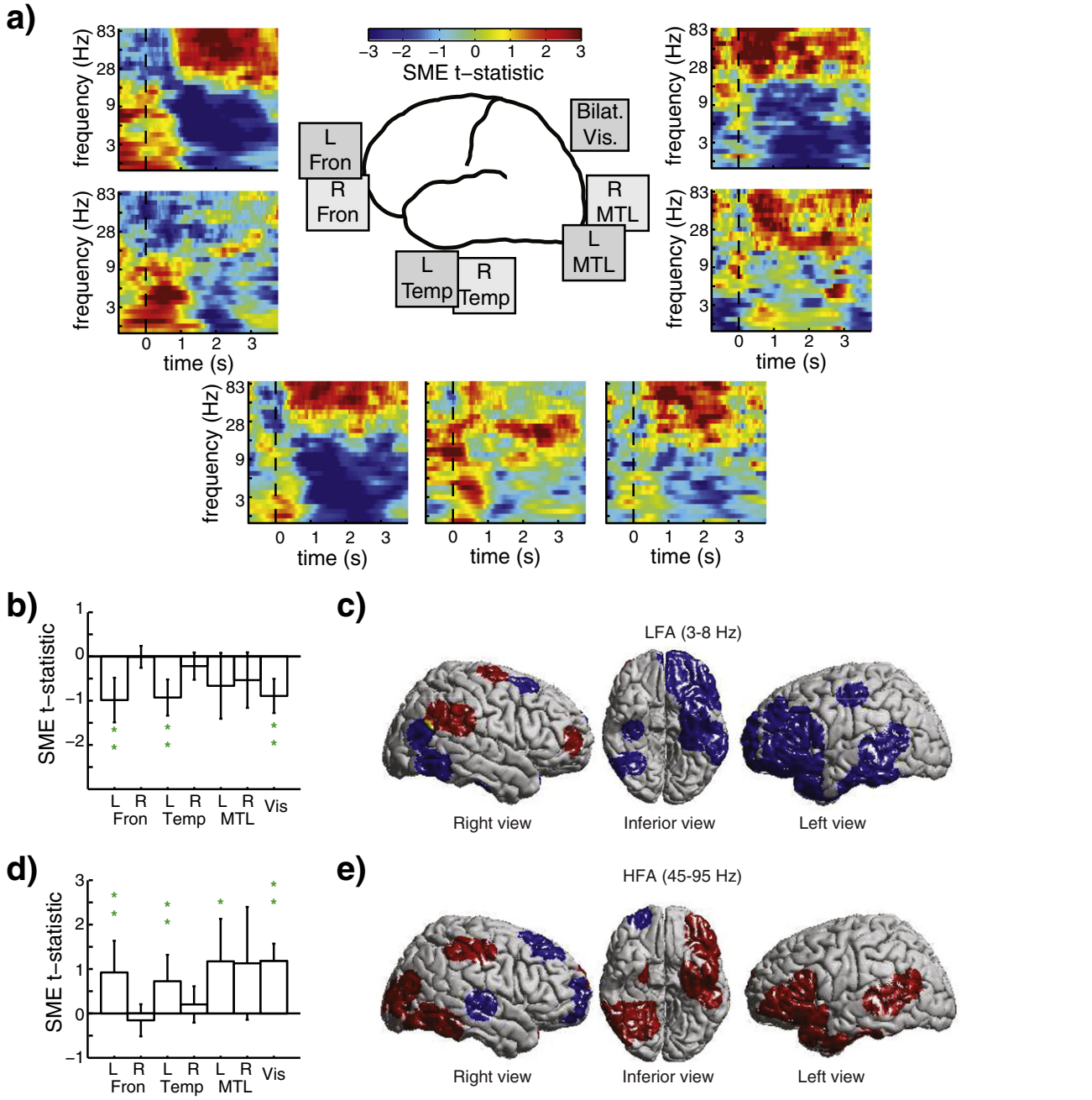

Fig. 2. a) Time frequency plots, showing across-subject average *t*-statistics for each anatomic region comparing successful to unsuccessful memory encoding. Frequencies are divided into 30 logarithmically-spaced bands ranging from 2 to 95 Hz. b) Average *t*-statistics across all participants for theta activity (3–8 Hz) for each anatomic region comparing successful to unsuccessful memory encoding. Regions exhibiting significant changes in LFA during successful encoding are represented with two green asterisks (FDR corrected; see Methods). Error bars represent standard error of the mean. c) Spatial ROIs exhibiting significant differences in LFA during successful memory encoding. Only ROIs exhibiting significant differences are colored. Blue and red represent significant (after correcting for multiple comparisons) decreases and increases in power, respectively. d) Average *t*-statistics across all participants for high frequency activity for each anatomic region comparing successful to unsuccessful memory encoding. Regions exhibiting significant changes in HFA during successful encoding are represented with two green asterisks (FDR corrected; see Methods). Error bars represent standard error of the mean. e) Spatial ROIs exhibiting significant differences in HFA during successful memory encoding.

Discussion

In order to directly examine the neural correlates of associative memory formation, we investigated iEEG spectral power during successful encoding as 27 participants performed a paired associates task. We examined LFA (3–8 Hz, theta) and HFA (45–95 Hz) and found that successful encoding was accompanied by broad decreases in LFA and corresponding increases in HFA. We found these changes most concentrated in the left temporal and frontal lobes and in the visual and MTL regions, although we also found smaller specific increases in LFA in the right temporal lobe and decreases in HFA in the right frontal lobe. We additionally found a temporal propagation of HFA increases from posterior to left anterior brain regions during successful memory encoding.

The changes in low and high frequency spectral power observed here are similar to previous analyses examining successful encoding during other verbal episodic memory tasks. In particular, successful encoding during a free recall task is characterized by an overall skew in power toward higher frequencies at the expense of lower frequencies, and a similar posterior to anterior progression of HFA (Burke et al., 2013,

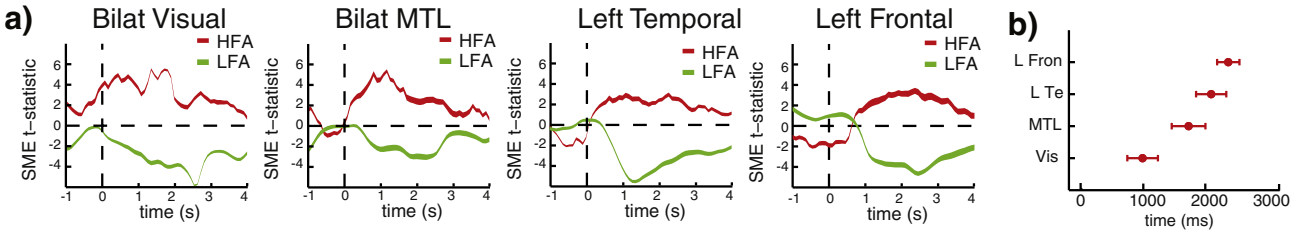

Fig. 3. a) Temporal evolution of the average HFA (red) and LFA (green) SME *t*-statistic across all participants in the bilateral visual, left MTL, left temporal, and left frontal lobe regions (see Methods). Line thickness represents standard error of the mean. b) The mean and SEM of the HFA peak times across all patients for each anatomic region. The curly brackets (with asterisks) represent timing differences between two regions where post-hoc *t*-tests revealed a significant difference (green color; $p < 0.01$) or a trend towards significance (black color; $p < 0.1$).

2014). The similarity in subsequent memory changes seen in both tasks is notable in that successful memory encoding in both tasks may rely on common cognitive processes. Computational models of memory encoding suggest that associative processes are critical for the type of encoding that supports later successful episodic memory retrieval (Kahana, 2012). The constrained nature of retrieval in the paired associates task contrasts with the highly unconstrained nature of retrieval in the free recall task (Underwood, 1945; Howard and Kahana, 2002; Polyn et al., 2009). In the latter, retrieval depends on the subjects ability to internally generate contextual cues to effectively search their memory. In contrast, the highly constrained nature of paired associates memory depends on the subject's ability to elaborate temporally defined associations among the concurrently processed list items.

Here we note a prominent decrease in LFA power during encoding. The observed decreases in theta activity have now been noted across many different studies of the electrophysiological correlates of human memory (Hanslmayr and Staudigl, 2013). This is surprising given the extensive animal literature demonstrating that hippocampal theta activity positively correlates with spatial memory formation. Rodent hippocampal theta organizes place cell firing and acts as a gate that selectively allows new information from the entorhinal cortex to reach the CA1 region of the hippocampus during encoding (Hasselmo and Stern, 2014). Given that rodent spatial memory is hypothesized to be the evolutionary origin of human episodic memory (Buzsaki and Moser, 2013), it is no wonder that the field has largely assumed that theta activity benefits memory formation (Klimesch et al., 1996; Molle et al., 2002; Sederberg et al., 2003; Hanslmayr et al., 2011; Lega et al., 2011; Caplan and Glaholt, 2007). This assumption is usually the starting point for many investigations regarding the neural correlates of human memory and, naturally, there has been a confirmation bias to detect positive increases in theta power during memory formation.

However, it has become clear that the single largest and most consistent electrophysiological effect that correlates with memory formation is a decrease in theta power (Sederberg et al., 2007; Guderian et al., 2009; Matsumoto et al., 2013; Burke et al., 2013, 2014). These decreases are present both in the hippocampus and in the neocortex. Although one possibility is that the observed theta decreases may be related to encoding mechanisms that benefit unconstrained retrieval during free recall (Hanslmayr and Staudigl, 2013), our data demonstrate robust decreases in LFA power during successful paired associates memory formation. Hence, theta decreases may reflect a more general process that marks memory formation irrespective of the retrieval process.

What do the decreases in theta activity tell us about how the brain forms episodic associations? Any interpretation will, at this point, remain speculative because there has not yet been an animal model to investigate these observed theta decreases in more detail. However, animal models in related behaviors that demonstrate similar decreases in theta power may provide some insight into why such decreases in theta activity may be important. Neural activity in mouse barrel cortex during active whisking involves a volley of information from thalamic neurons, which leads to pronounced decrease in theta power in this cortical region (Poulet and Petersen, 2008; Poulet et al., 2012). These decreases were traced to a reduced correlation between individual neurons, which may enable more efficient local computation (Harris and Thiele, 2011). Hence, one possibility is that the decreases in theta activity that we observe during episodic encoding may reflect decreases in neuronal correlations across the cortex and the medial temporal lobe, increasing the amount of information that can be stored in the overall network.

Our data also demonstrate that HFA increases during the successful formation of associations. HFA has been linked to underlying multi-unit activity (Manning et al., 2009; Ray and Maunsell, 2011a) and likely reflects large scale increases in neural firing in the many thousands of neurons beneath the intracranial electrode (Miller et al., 2009). HFA can therefore be considered as a surrogate for general neural activation and, when elevated, suggests that part of the brain is participating in memory formation (Burke et al., 2015). Indeed, the increases in HFA observed here are consistent with previous studies reporting increases in left temporal lobe multi-unit activity during the formation of word–word pairs during a paired associates task (Ojemann and Schoenfield-McNeill, 1998).

Our data suggest that HFA propagates across the cortex in an overall posterior to anterior direction during memory encoding. This result is similar to previous studies of encoding that have also shown a highly conserved spatiotemporal propagation of HFA during encoding (Burke et al., 2013, 2014). However, despite the clear progression of HFA during encoding, it is unclear what such activity represents. One possibility is that the HFA posterior to anterior progression may be phase-locked to a lower frequency traveling wave that, together, transmits information across the cortex. This mechanism has been shown in human intracranial recordings to transmit gamma burst activity at a rate of 0.7 to 2.1 m/s (Bahramisharif et al., 2013). The functional role of traveling waves in memory processing remains an open question.

In this manuscript, we were interested in the formation of new associations, as reflected by neural activity in the post-stimulus time interval. However, we make two additional notes. First, recent work has pointed to the importance of particular cognitive states in the encoding of new associations, as reflected by activity in the pre-stimulus time interval (Guderian et al., 2009; Merkow et al., 2014). Because the neural correlates of pre- and post-stimulus activity have been shown to be inversely proportional (see Supplemental Fig. 2, Fell et al., 2011), we suggest that the cognitive operations reflected by these activations are distinct. Second, recent evidence has suggested that LFA and HFA are not independent, and can interact with one another through phase-amplitude coupling (Bahramisharif et al., 2013). Whether such phase amplitude coupling is directly related to associative memory encoding and is linked to the observed changes in power remains a question for future investigation.

In conclusion, we find that the observed changes in LFA and HFA with successful memory encoding during a paired associates memory task, similar to patterns observed in other episodic memory paradigms, may reflect the neural mechanisms underlying the formation of associations. The decreases in LFA, increases in HFA, and progression of HFA activity from posterior to left anterior regions of the brain underlie a

common memory encoding mechanism that is conserved across multiple tasks. Because paired associates memory formation relies on the retrieval of explicit associations between items, these electrophysiological patterns likely do not reflect neural mechanisms mediating memory formation that only benefit subsequent retrieval using internally generated contextual cues (Staudigl and Hanslmayr, 2013). In this case, this pattern of activity would be exclusive to free recall. Instead, we find that decreases in LFA and increases in HFA are also observed during successful paired associates memory encoding, and therefore may reflect a common neural mechanism mediating the successful formation of associations.

Funding

This work was supported by the National Institutes of Health Intramural Research Program and by NIH grants MH055687, MH061975, NS067316, and MH017168.

Acknowledgments

We thank Dale H. Wyeth and Edmund Wyeth for technical assistance at Thomas Jefferson Hospital. The authors declare no competing financial interests. We are indebted to all patients who have selflessly volunteered their time to participate in our study.

References

Addison, P.S., 2002. The Illustrated Wavelet Transform Handbook: Introductory Theory and Applications in Science, Engineering, Medicine and Finance. Institute of Physics Publishing, Bristol.
Anderson, K.L., Rajagovindan, R., Ghacibeh, G., Meador, K.J., Ding, M., 2010. Theta oscillations mediate interaction between prefrontal cortex and medial temporal lobe in human memory. Cereb. Cortex 7, 1604–1612.
Bahramisharif, A., van Gerven, M.A., Aarnoutse, E.J., Mercier, M.R., Schwartz, T.H., Foxe, J.J., Jensen, O., 2013. Propagating neocortical gamma bursts are coordinated by traveling alpha waves. J. Neurosci. 33 (48), 18849–18854.
Burke, J.F., Zaghloul, K.A., Jacobs, J., Williams, R.B., Sperling, M.R., Sharan, A.D., Kahana, M.J., 2013. Synchronous and asynchronous theta and gamma activity during episodic memory formation. J. Neurosci. 1, 292–304.
Burke, J.F., Long, N.M., Zaghloul, K.A., Sharan, A.D., Sperling, M.R., Kahana, M.J., 2014. Human intracranial high-frequency activity maps episodic memory formation in space and time. NeuroImage 2, 834–843.
Burke, J.F., Ramayya, A.G., Kahana, M.J., 2015. Human intracranial high-frequency activity during memory processing: neural oscillations or stochastic volatility? Curr. Opin. Neurobiol. 31, 104–110.
Buzsaki, G., Moser, E.I., 2013. Memory, navigation and theta rhythm in the hippocampal-entorhinal system. Nat. Neurosci. 16 (2), 130–138.
Caplan, J.B., 2005. Associative isolation: unifying associative and list memory. J. Math. Psychol. 49, 383–402.
Caplan, J.B., Glaholt, M., 2007. The roles of EEG oscillations in learning relational information. NeuroImage 5, 604–616.
Dalton, M., Tu, S., Hornberger, M., Hodges, J., Piguet, O., 2013. Medial temporal lobe contributions to intra-item associative recognition memory in the aging brain. Front. Behav. Neurosci. 7, 222.
Davachi, L., Mitchell, J.P., Wagner, A.D., 2003. Multiple routes to memory: distinct medial temporal lobe processes build item and source memories. PNAS 4, 2157–2162.
Fell, J., Ludowig, E., Staresina, B.P., Wagner, T., Kranz, T., Elger, C.E., Axmacher, N., 2011. Medial temporal theta/alpha power enhancement precedes successful memory encoding: evidence based on intracranial EEG. J. Neurosci. 31 (14), 5392–5397.
Genovese, C.R., Lazar, N.A., Nichols, T.E., 2002. Thresholding of statistical maps in functional neuroimaging using the false discovery rate. NeuroImage 15, 870–878.
Guderian, S., Schott, B., Richardson-Klavehn, A., Duzel, E., 2009. Medial temporal theta state before an event predicts episodic encoding success in humans. PNAS 13, 5365.
Hanslmayr, S., Staudigl, T., 2013. How brain oscillations form memories—a processing based perspective on oscillatory subsequent memory effects. NeuroImage 5, 326–334.
Hanslmayr, S., Volberg, G., Wimber, M., Raabe, M., Greenlee, M.W., B¨aumel KHT,, 2011. The relationship between brain oscillations and bold signal during memory formation: a combined EEG-FMRI study. J. Neurosci. 44, 15674–15680.
Harris, K.D., Thiele, A., 2011. Cortical state and attention. Nat. Rev. Neurosci. 12 (9), 509–523.
Hasselmo, M.E., Stern, C.E., 2014. Theta rhythm and the encoding and retrieval of space and time. Neuroimage 85 (2014), 656–666.
Howard, M.W., Kahana, M.J., 2002. A distributed representation of temporal context. J. Math. Psychol. 46, 269–299.
Jacobs, J., Kahana, M.J., 2010. Direct brain recordings fuel advances in cognitive electrophysiology. Trends Cogn. Sci. 4, 162–171.
Kahana, M.J., 2012. Foundations of Human Memory. Oxford University Press, New York, NY.
Klimesch, W., Doppelmayr, M., Russegger, H., Pachinger, T., 1996. Theta band power in the human scalp EEG and the encoding of new information. Neuroreport 7, 1235–1240.
Kovach, C.K., Tsuchiya, N., Kawasaki, H., Oya, H., Howard III, M.A., Adolphs, R., 2011. Manifestation of ocular-muscle emg contamination in human intracranial recordings. Neuroimage 1, 213–233.
Lancaster, J.L., Woldorff, M.G., Parsons, L.M., Liotti, M., Freitas, C.S., Rainey, L., Fox, P.T., 2000. Automated Talairach atlas labels for functional brain mapping. Hum. Brain Mapp. 3, 120–131.
Lega, B., Jacobs, J., Kahana, M.J., 2011. Human hippocampal theta oscillations and the formation of episodic memories. Hippocampus 4, 748–761.
Magri, C., Schridde, U., Murayama, Y., Panzeri, S., Logothetis, N.K., 2012. The amplitude and timing of the bold signal reflects the relationship between local field potential power at different frequencies. J. Neurosci. 4, 1395–1407.
Manning, J.R., Jacobs, J., Fried, I., Kahana, M.J., 2009. Broadband shifts in LFP power spectra are correlated with single-neuron spiking in humans. J. Neurosci. 43, 13613–13620.
Manning, J.R., Polyn, S.M., Baltuch, G., Litt, B., Kahana, M.J., 2011. Oscillatory patterns in temporal lobe reveal context reinstatement during memory search. PNAS 31, 12893–12897.
Matsumoto, J.Y., Stead, M., Kucewics, M.T., Matsumoto, A.J., Peters, P.A., Brinkmann, B.H., Worrell, G.A., 2013. Network oscillations modulate interictal epileptiform spike rate during human memory. Brain 8, 2444–2456.
Mayes, A.R., Montaldi, D., Migo, E., 2007. Associative memory and the medial temporal lobes. Trends Cogn. Sci. 3, 126–135.
McClelland, J.L., McNaughton, B.L., O'Reilly, R.C., 1995. Why there are complementary learning systems in the hippocampus and neocortex: insights from the successes and failures of connectionist models of learning and memory. Psychol. Rev. 3, 419–457.
Merkow, M.B., Burke, J.F., Stein, J., Kahana, M.J., 2014. Prestimulus theta in the human hippocampus predicts subsequent recognition but nor recall. Hippocampus 24, 1562–1569.
Miller, K.J., Zanos, S., Fetz, E.E., den Nijs, M., Ojemann, J., 2009. Decoupling the cortical power spectrum reveals real-time representation of individual finger movements in humans. J. Neurosci. 10, 3132–3137.
Molle, M., Marshall, L., Fehm, H.L., Born, J., 2002. EEG theta synchronization conjoined with alpha desynchronization indicate intentional encoding. Eur. J. Neurosci. 5, 923–928.
Mukamel, R., Gelbard, H., Arieli, A., Hasson, U., Fried, I., Malach, R., 2005. Coupling between neuronal firing, field potentials, and fMRI in human auditory cortex. Science 5736, 951–954.
Norman, K.A., O'Reilly, R.C., 2003. Modeling hippocampal and neocortical contributions to recognition memory: a complementary learning systems approach. Psychol. Rev. 110, 611–646.
Nunez, P.L., Srinivasan, R., 2006. Electric Fields of the Brain. Oxford University Press, New York.
Nyhus, E., Curran, T., 2010. Functional role of gamma and theta oscillations in episodic memory. Neurosci. Biobehav. Rev. 7, 1023–1035.
Ojemann, G.A., Schoenfield-McNeill, J., 1998. Neurons in human temporal cortex active with verbal associative learning. Brain Lang. 3, 317–327.
Paller, K.A., Wagner, A.D., 2002. Observing the transformation of experience into memory. Trends Cogn. Sci. 2, 93–102.
Polyn, S.M., Norman, K.A., Kahana, M.J., 2009. A context maintenance and retrieval model of organizational processes in free recall. Psychol. Rev. 1, 129–156.
Poulet, J.F., Petersen, C.C., 2008. Internal brain state regulates membrane potential synchrony in barrel cortex of behaving mice. Nature 454 (7206), 881–885.
Poulet, J.F., Fernandez, L.M., Crochet, S., Petersen, C.C., 2012. Thalamic control of cortical states. Nat. Neurosci. 15 (3), 370–372.
Ray, S., Maunsell, J., 2011a. Different origins of gamma rhythm and high-gamma activity in macaque visual cortex. PLoS Biol. 4.
Ray, S., Maunsell, J., 2011b. Network rhythms influence the relationship between spike-triggered local field potential and functional connectivity. J. Neurosci. 35, 12674–12682.
Sederberg, P.B., Kahana, M.J., Howard, M.W., Donner, E.J., Madsen, J.R., 2003. Theta and gamma oscillations during encoding predict subsequent recall. J. Neurosci. 34, 10809–10814.
Sederberg, P.B., Schulze-Bonhage, A., Madsen, J.R., Bromfield, E.B., McCarthy, D.C., Brandt, A., Kahana, M.J., 2007. Hippocampal and neocortical gamma oscillations predict memory formation in humans. Cereb. Cortex 5, 1190–1196.
Serruya, M.D., Sederberg, P.B., Kahana, M.J., 2014. Power shifts track serial position and modulate encoding in human episodic memory. Cereb. Cortex 24, 403–413.
Staudigl, T., Hanslmayr, S., 2013. Theta oscillations at encoding mediate the context-dependent nature of human episodic memory. Curr. Biol. 12, 1101–1106.
Underwood, B.J., 1945. The effect of successive interpolations and proactive inhibition. Psychol. Monogr. 59.